GaN/AlGaN ultraviolet/infrared dual-band detector

G. Ariyawansa, M. B. M. Rinzan, M. Alevli, M. Strassburg, N. Dietz, and A. G. U. Perera[a)]
Department of Physics and Astronomy, Georgia State University, Atlanta, Georgia 30303

S. G. Matsik
NDP Optronics, Mableton, Georgia 30126

A. Asghar and I. T. Ferguson
School of Electrical and Engineering, Georgia Institute of Technology, Atlanta, Georgia 30332

H. Luo, A. Bezinger, and H. C. Liu
Institute for Microstructural Sciences, National Research Council, Ottawa K1A OR6, Canada

(Received 19 May 2006; accepted 10 July 2006; published online 30 August 2006)

Group III-V wide band gap materials are widely used in developing solar blind, radiation-hard, high speed optoelectronic devices. A device detecting both ultraviolet (UV) and infrared (IR) simultaneously will be an important tool in fire fighting and for military and other applications. Here a heterojunction UV/IR dual-band detector, where the UV/IR detection is due to interband/intraband transitions in the $Al_{0.026}Ga_{0.974}N$ barrier and GaN emitter, respectively, is reported. The UV threshold observed at 360 nm corresponds to the band gap of the $Al_{0.026}Ga_{0.974}N$ barrier, and the IR response obtained in the range of 8–14 μm is in good agreement with the free carrier absorption model. © *2006 American Institute of Physics*. [DOI: 10.1063/1.2345226]

During the last decades, there has been an extensive increase in the demand for developing high speed electronic and optoelectronic devices based on group III nitrides. Ultraviolet (UV) detectors,[1,2] UV light emitting diodes,[3–5] and laser diodes[6] have been successfully demonstrated and are widely available for commercial applications such as flame detection, UV imaging, solar UV detection, as well as applications for industries such as those focusing on military, agricultural, and automotive products. Researchers have reported GaN/AlGaN Schottky photodiodes[7] and quantum well infrared photodetectors[8] operating in near-/midinfrared (NIR/MIR) regions. However, development of GaN high speed optoelectronic devices with improved performance is still in its infancy since the growth of high-quality GaN/AlGaN heterostructures is limited by the availability of suitable lattice-matched substrate materials and process/material knowledge base. In this letter, a heterojunction interfacial workfunction internal photoemission (HEIWIP) detector based on GaN/AlGaN heterostructure, which can be operated in both UV and IR (8–14 μm) regions, is reported. Detecting multiple wave bands by a single detector can eliminate the difficulties of assembling several detectors with separate cooling assemblies and electronics. So far, several dual-band detectors[9–11] based on group-III–As material system, operating in NIR and MIR/far-infrared (FIR) regions, have been reported. GaN dual-band detectors[12] reported so far can detect UV and NIR radiations. UV/IR dual-band detectors could be used in applications where the detection of both the UV and IR radiations is important. For example, fire and flame detection where fires emit radiation from UV to IR and different flames such as hydrogen and coal have significant intensity variation in the emission spectrum in the UV and IR regions.

The HEIWIP structure was grown by organometallic chemical vapor deposition on sapphire substrate and consists of a n^+ GaN emitter layer (also served as the top contact), an undoped $Al_{0.026}Ga_{0.974}N$ barrier, and a GaN n^+ bottom contact layer, as shown in Fig. 1(a). The sample was annealed under a N_2 gas flow at 700 °C for 2 min.

The dual-band detection mainly involves two detection mechanisms. The UV detection is based on interband transitions of carriers in the $Al_{0.026}Ga_{0.974}N$ barrier, while the IR detection is due to intraband transitions of free carriers in the emitter. The energy band diagram indicating the transitions due to both mechanisms is depicted in Fig. 1(b). The intraband detection (IR) mechanism involves free carrier absorption in the emitter, followed by the internal photoemission of photoexcited carriers across the junction barrier, and then the collection of carriers by the applied electric field at the contacts. The offset between the Fermi level in the emitter layer and the valance band edge of the barrier layer forms the interfacial work function (Δ), which arises due to the band offset of different materials[13] and the band gap narrowing[14] of the highly doped emitter layer. The threshold wavelength λ_0 (in micrometers) is given by $1240/\Delta$, where Δ is in meV.

Current-voltage (*IV*) measurements were carried out by using a Keithley 2400 source meter. The dark *IV* character-

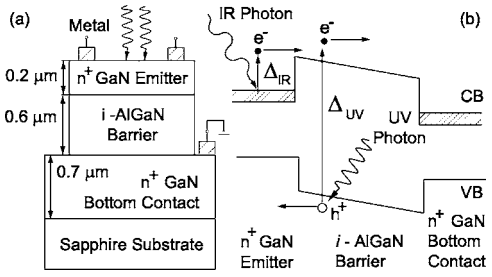

FIG. 1. (a) Schematic diagram of GaN/AlGaN HEIWIP structure. The emitter (top contact) and the bottom contact are doped to 5×10^{18} cm^{-3} with Si as the *n*-type dopant, while the $Al_{0.026}Ga_{0.974}N$ barrier is not intentionally doped. (b) The band diagram showing the conduction/valence band profile of the structure and the transitions leading to UV and IR responses.

[a)]Electronic mail: uperera@gsu.edu

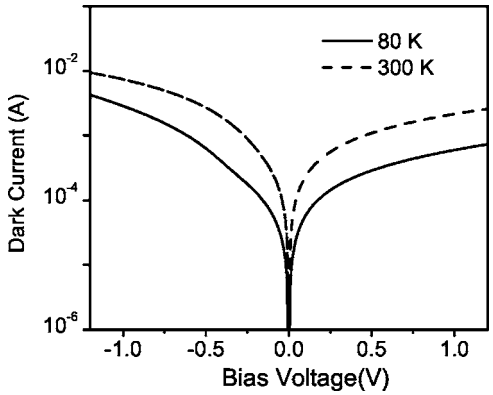

FIG. 2. Dark current of the detector at 80 and 300 K. The higher dark current of the detector compared to other detectors operating in similar regions is possibly ascribed to hopping conductivity of Si impurity electrons in the barrier.

istics of the detector are shown in Fig. 2. The higher dark current of the detector compared to other detectors operating in the similar regions is possibly ascribed to hopping conductivity of Si impurity electrons in the barrier. The presence of Si impurities has been confirmed by the response peaks corresponding to impurity photoionization of impurity atoms, which is discussed later.

The UV/IR dual-band response of the sample is shown in Fig. 3(a). The UV spectra were obtained using an Oriel Deuterium UV source, UV/visible (VIS) monochromator, and neutral density filters, and spectra were calibrated using a background spectrum obtained by a Hamamatsu photomultiplier tube with a known sensitivity. As shown in Fig. 1(b), UV photons excite the valance electrons in the $Al_{0.026}Ga_{0.974}N$ barrier layer, and the generated electron-hole pairs are separated by the applied electric field before recombination. The UV threshold wavelength observed at 360 nm matches the band gap of $Al_{0.026}Ga_{0.974}N$ alloy. The IR spectral response of the detector was obtained for normal incidence radiation using a Perkin Elmer System 2000 Fourier transform infrared spectrometer. The spectra were calibrated by using a background spectrum obtained with a Si composite bolometer with the same set of optical components. The free carrier absorption occurs in the emitter layer and carriers undergo photoemission across the barrier [Fig. 1(b)]. The detector shows a 14 μm free carrier threshold and peaks at 12 μm.

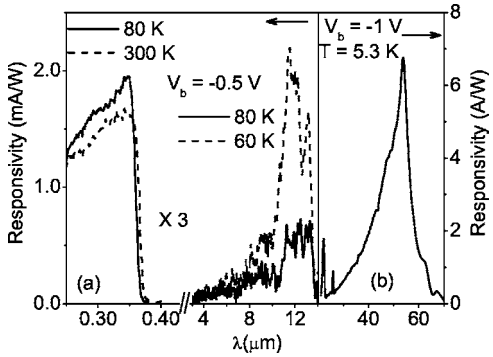

FIG. 3. (a) UV/IR dual-band response of the detector. The IR response is visible at 80 K, while the UV response can be obtained even above 300 K. (b) The response at 54 μm (5.5 THz) which is due to the transition between 1*s* and 2*p*± impurity levels of Si in GaN.

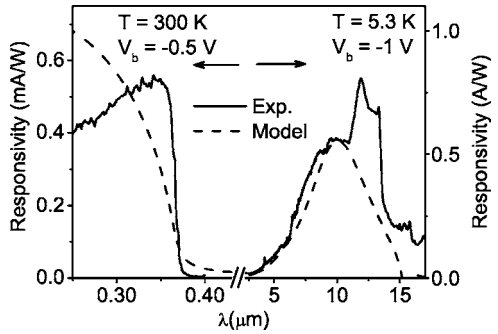

FIG. 4. Calculated UV/IR responses (dashed line) of the detector, fitted with experimental results (solid line). The IR response consists of a free carrier response, which matches with the calculated response, and an impurity-related response.

The experimental responsivities of the detector in both UV and IR regions are fitted to theoretically expected responses, as shown in Fig. 4. The calculation is based on a model[13] in which the complex permittivities for interband and intraband transitions are calculated using the model dielectric function[15] and the Lorentz-Drude theory, respectively. The light propagation in the structure is derived from the transfer matrix method. The responsivity R is given by $R=\eta g_p q\lambda/hc$, where η is the total quantum efficiency, g_p is the photoconductive gain, q is the electron charge, λ is the wavelength, h is Planck's constant, and c is the speed of light. The enhanced UV response near the band edge is probably due to high carrier concentration near the band edge, which is not taken into account in the model. The IR response consists of a free carrier response, which matches with the calculated response, and an impurity-related response.

The broad peak in the 11–13.6 μm region superimposed on the free carrier response is tentatively assigned to transitions related to carbon or nitrogen states. The reported donor ionization energy of carbon[16] falls in the 110–140 meV range, while the binding energy of N vacancy[17] is about 100 meV. Assuming that the two peaks observed at 11.9 μm (104.2 meV) and 13.3 μm (93.2 meV) are due to transitions of excited carbon states, the ionization energies were calculated to be 139 and 124 meV, respectively. These ionization energy values in the 140–110 meV range support the assumption that the corresponding transitions are carbon donor related impurity transitions.

As shown in Fig. 3(b), a sharp peak at 54 μm (5.5 THz) is observed in the response spectrum. The corresponding energy for transitions leading to this peak is 23 meV. Wang *et al.*[18] reported that the donor binding energy of Si in GaN is 29 meV, and the transition from 1*s* to 2*p*± level occurs at 21.9 meV. Moore *et al.*[19] reported the 1*s*-2*p*± transition of Si in GaN at 23.3 meV and donor effective mass binding energy of 31.1 meV. Hence, it is concluded that the sharp response peak observed at 23 meV can be identified as 1*s*-2*p*± transition of Si donors in GaN. As evident from the results, GaN provides the advantage of developing a 5.5 THz (54 μm) detector, based on the 1*s*-2*p*± transition of Si in GaN. On the other hand, the Si impurity-related transition can lead to an increased dark current for a detector designed to operate in a shorter wavelength region.

The dual-band detection approach, reported in this letter, can be used to develop dual-band detectors tailored to spe-

cific applications. By adjusting the material composition in the layers, the thresholds for the interband and intraband responses can be tailored separately. For example, in an AlGaN based detector, if the Al fraction is varied in both the emitter and barrier by the same amount, only the interband threshold will change, while the intraband threshold remains constant. Alternatively, varying only the emitter Al fraction, the intraband threshold could be varied without changing the interband threshold. Moreover, the resonant cavity effects can be used to tailor the IR response peak to the desired wavelength. By adjusting the materials, it will be possible to tune the interband threshold from the UV to NIR and the intraband threshold from the MIR to FIR. That is, the reported dual-band approach with HEIWIP detectors can be tested with any material such as InN, InGaN, GaN, AlGaN, and AlN. InN could give an interband response in the NIR region, while InGaN could respond in the VIS-NIR regions. A UV interband response could be expected from an AlN based detector. Bias voltage could select the required operating regions, UV-IR, VIS-IR, or UV-VIS. Also, as the response for the two processes originates at different locations, it will be possible to design a device that is capable of separately measuring both components simultaneously. The idea is to use three contacts to measure two separate currents simultaneously and then, from these currents, to separate the UV and IR contributions. Furthermore, different designs to increase the performance of the detector have to be studied.

In summary, a GaN/AlGaN HEIWIP dual-band detector responding in UV and IR regions based on interband and intraband transitions in the structure is reported. The UV threshold is observed at 360 nm and the IR response is in the $8-14$ μm region. By adjusting the material or the alloy fraction, the threshold of the interband and intraband responses can be tailored. Based on theoretical models and experimental data, the transitions leading to each band are explained. The detector also demonstrates the development of detectors responding in several wavelength regions by changing the material system.

This work is supported in part by the U.S. Air Force Small Business Innovation Research Program (SBIR) under Grant No. FA9453-05-M-0106. The authors would like to acknowledge Dave Cardimona and Tzveta Apostolova for fruitful discussions and the support and Rongzhu Wang and Hun Kang for technical assistance.

[1] M. Asif Khan, J. N. Kuznia, D. T. Olson, M. Blasingame, and A. R. Bhattarai, Appl. Phys. Lett. **63**, 2455 (1993).
[2] D. Walker, X. Zhang, P. Kung, A. Saxler, S. Javadpour, J. Xu, and M. Razeghi, Appl. Phys. Lett. **68**, 2100 (1996).
[3] Madalina Furis, A. N. Cartwright, Hong Wu, and William J. Schaff, Appl. Phys. Lett. **83**, 3486 (2003).
[4] S. K. Zhang, W. B. Wang, I. Shtau, F. Yun, L. He, H. Morko, X. Zhou, M. Tamargo, and R. R. Alfano, Appl. Phys. Lett. **81**, 4862 (2002).
[5] J. P. Zhang, X. Hu, Yu. Bilenko, J. Deng, A. Lunev, M. S. Shur, R. Gaska, M. Shatalov, J. W. Yang, and M. A. Khan, Appl. Phys. Lett. **85**, 5532 (2004).
[6] V. D. Jovanovic, D. Indjin, Z. Ikonic, and P. Harrison, Appl. Phys. Lett. **84**, 2995 (2004).
[7] N. Biyikli, T. Kartaloglu, O. Aytur, I. Kimukin, and E. Ozbay, MRS Internet J. Nitride Semicond. Res. **8**, 2 (2003).
[8] Claire Gmachl, Hock M. Ng, and Alfred Y. Cho, Appl. Phys. Lett. **77**, 334 (2000).
[9] Arnold Goldberg, Parvez N. Uppal, and Michael Winn, Infrared Phys. Technol. **44**, 427 (2003).
[10] H. C. Liu, C. Y. Song, A. Shen, M. Gao, Z. R. Wasilewski, and M. Buchanan, Appl. Phys. Lett. **77**, 2437 (2000).
[11] M. P. Touse, G. Karunasiri, K. R. Lantz, H. Li, and T. Mei, Appl. Phys. Lett. **86**, 093501 (2005).
[12] D. Starikov, C. Boney, R. Pillai, and A. Bensaoula, *Proceedings the ISA/EEE Sensors for Industry Conference 2004, New Orleans, LA, 2004* (IEEE, Piscataway, NJ, 2004), pp. 36–40.
[13] D. G. Esaev, M. B. M. Rinzan, S. G. Matsik, and A. G. U. Perera, J. Appl. Phys. **96**, 4588 (2004).
[14] W. Z. Shen, A. G. U. Perera, H. C. Liu, M. Buchanan, and W. J. Schaff, Appl. Phys. Lett. **71**, 2677 (1997).
[15] Takahiro Kawashima, Hisashi Yoshikawa, Sadao Adachi, Shunro Fuke, and Kohji Ohtsuka, J. Appl. Phys. **82**, 3528 (1997).
[16] V. Bougrov, M. Levinshtein, S. Rumyantsev, and A. Zubrilov, in *Properties of Advanced SemiconductorMaterials GaN, AlN, InN, BN, SiC, SiGe*, edited by M. E. Levinshtein, S. L. Rumyantsev, and M. S. Shur (Wiley, New York, 2001), p. 1.
[17] M. Sumiya, K. Yoshimura, K. Ohtsuka, and S. Fuke, Appl. Phys. Lett. **76**, 2098 (2000).
[18] Y. J. Wang, R. Kaplan, H. K. Ng, K. Doverspike, D. K. Gaskill, T. Ikedo, I. Akasaki, and H. Amono, J. Appl. Phys. **79**, 8007 (1996).
[19] W. J. Moore, J. A. Freitas, Jr., and R. J. Molnar, Phys. Rev. B **56**, 12073 (1997).